16th World Conference on Earthquake Engineering, 16WCEE 2017
Santiago Chile, January 9th to 13th 2017
Paper N° 1098
Registration Code: S-C1463192992

A PRACTICAL APPLICATION OF THE NONLINEAR SUBSTRUCTURING CONTROL METHOD TO BASE-ISOLATED STRUCTURES

R. Enokida(1) and K. Kajiwara(2)

(1) Research fellow, E-Defense, National Research Institute for Earth Science and Disaster Prevention,enokida@bosai.go.jp
(2) Director, E-Defense, National Research Institute for Earth Science and Disaster Prevention,kaji@bosai.go.jp

Abstract

A dynamical substructuring system (DSS) is a substructuring methodology where a dynamical experiment is implemented on a physical substructure, plus real-time interaction with a simulated numerical substructure. The linear substructuring control (LSC) method is a control law specifically designed for DSS, requiring knowledge of the nominal dynamics of the substructures as well as actuation (i.e. transfer) system. Therefore, application of the LSC method alone is limited to relatively well-known systems. In this study, we propose a nonlinear substructuring control (NLSC) as a more general form of LSC by incorporating a nonlinear signal-based control (NSBC) method into DSS. Although the LSC controller requires properties of substructured systems, the newly developed NLSC controller does not relies on such accurate properties, because of the implementation of NSBC. NLSC here is numerically and experimentally examined in a comparison with LSC, via a substructuring test on a rubber bearing, commonly used in base-isolated structures. In the examinations, stiffness of the rubber bearing used in the LSC and NLSC controllers is deliberately assumed to be five times as large as the real value. In substructuring experiments conducted with a rubber bearing and a hydraulic actuator, NLSC achieved accurate control with very small error even with the inaccurate assumption, while LSC showed 15 times larger error. NLSC is found to be effective in executing substructured experiments containing poorly known parameters in the substructures.

Keywords: Nonlinear signal-based control, dynamically substructured system, nonlinear substructuring control, rubber bearing.

1. Introduction

Dynamical substructure testing, whereby a dynamical experiment is conducted upon a critical part (referred to as the *physical substructure*) of an emulated system with real-time simulations of the other parts (referred to as the *numerical substructure*) of the system, has become a key experimental method in a wide range of engineering fields. The purpose is to study the properties of the critical part, such as its nonlinear characteristics, instead of conducting dynamical experiments on the entire emulated system. Therefore, the dynamical substructuring methodology is required to maintain robustness for systems having nonlinearity or uncertainty.

The dynamically substructured system (DSS), proposed from the perspective of automatic control system design [1], generates an input signal to the transfer system (a combination of actuators, inner-loop controllers and signal-conditioning hardware) that drives the physical substructure output so that it closely matches that of the corresponding output of the numerical substructure. In this method, knowledge of the parameters of the substructures as well as the transfer system is required in the formulation of the DSS using a linear substructuring controller (LSC). The advantage of the DSS-LSC strategy is the resultant separation of the emulated system dynamics from those of the closed-loop error dynamics. This enables the representation of even very lightly damped emulated systems using a DSS configuration with large stability margins that are designed into the system. However, the applicability of LSC is limited to relatively well-known systems because it is designed on the basis of the dynamics of the substructures. As a result, adaptive minimal control synthesis [1, 2, 3] is required in the DSS scheme when system parameters are unknown or poorly known. In this study, we propose a nonlinear substructuring control (NLSC) method as a generalised form of LSC by incorporating a recently developed nonlinear signal-based control (NSBC) [4] to handle poorly known systems. We examine

NLSC in numerical and experimental studies of a substructured test on a rubber bearing used in base-isolated structure, as shown in Fig. 1.

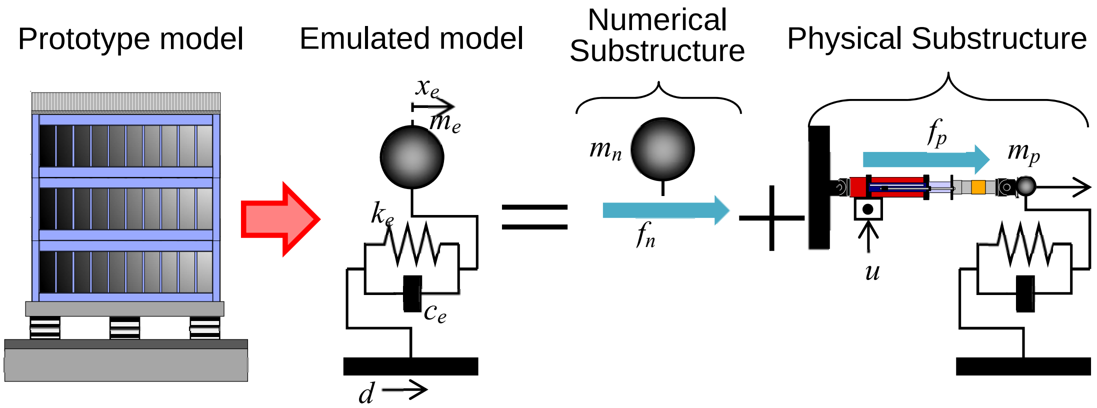

Fig. 1 – Dynamical substructuring test of a base-isolated structure with a rubber bearing

2. Nonlinear substructuring control

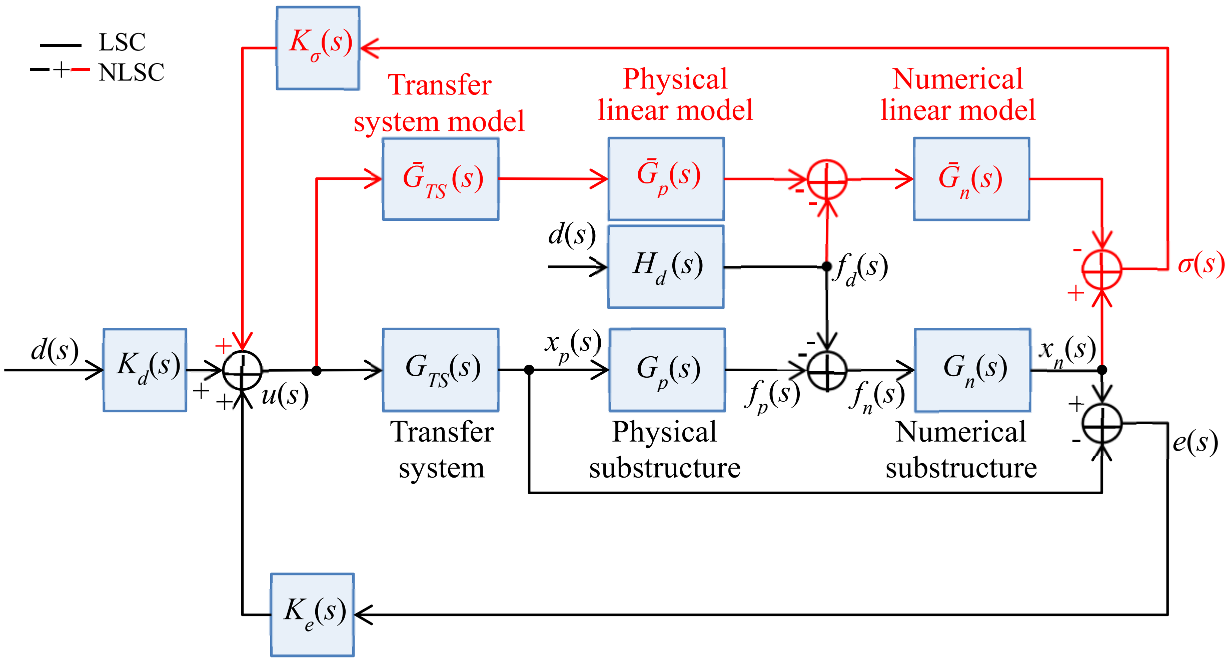

Fig. 2 – Nonlinear substructuring control

NSBC manages nonlinear systems based on a nonlinear signal [4], and this method can be incorporated into substructuring tests when a signal corresponding to the nonlinear signal is given. Thus, NLSC shown in Fig. 2 is developed as an application of NSBC. In this method, a transfer system, which is crucially important for the interaction between the physical and numerical substructures, and its model are assumed to be:

$$\begin{cases} G_{TS}(s) = G_{ts}(s)e^{-\tau s} \\ \bar{G}_{TS}(s) = \bar{G}_{ts}(s)e^{-\tau s} \end{cases} \tag{1}$$

where G_{TS} and G_{ts} represent the transfer system dynamics including a pure time delay τ, and the un-delayed component of the transfer system dynamics, respectively, and $\bar{G}_{TS}$ and $\bar{G}_{ts}$ represent those linear models.

In NLSC, substructures are expressed by:

$$\begin{cases} G_p(s) = \bar{G}_p(s) + \Delta G_p(s) \\ G_n(s) = \bar{G}_n(s) + \Delta G_n(s) \end{cases} \tag{2}$$

where G_p and G_n are the physical and numerical substructures, $\bar{G}_p$ and $\bar{G}_n$ are the linear models of the substructures, and ΔG_p and ΔG_n are the nonlinearities of the substructures. Output forces from the nonlinear physical substructure and its linear model in Fig. 2 can be expressed by:

$$\begin{cases} f_p(s) = G_p(s) G_{TS}(s) u(s) \\ \bar{f}_p(s) = \bar{G}_p(s) \bar{G}_{TS}(s) u(s) \end{cases} \tag{3}$$

where $\bar{f}_p$ is the force generated in the physical linear model and f_p is the force generated in the physical substructure. Outputs from the numerical substructure and its linear model can be expressed by:

$$\begin{cases} x_n(s) = G_n(s)\left(-f_p(s) - f_d(s)\right) \\ \bar{x}_n(s) = \bar{G}_n(s)\left(-\bar{f}_p(s) - f_d(s)\right) \end{cases} \tag{4}$$

where f_d is the force related to the disturbance d.

The nonlinear signal in NLSC is defined to be:

$$\sigma(s) = x_n(s) - \bar{x}_n(s) \tag{5}$$

When the dynamics of the transfer system are well known, the outputs of the transfer system and its model are nearly identical. Based on this assumption of $x_p(s) = \bar{x}_p(s)$, the outputs of the substructures can be rewritten as:

$$\begin{cases} x_n(s) = \bar{x}_n(s) + \sigma(s) = \bar{G}_1(s) f_d(s) - \bar{G}_0(s) e^{-\tau s} u(s) + \sigma(s) \\ x_p(s) = \bar{x}_p(s) = \bar{G}_2(s) e^{-\tau s} u(s) \end{cases} \tag{6}$$

where $\bar{G}_1(s) = -\bar{G}_n(s) H_d(s), \bar{G}_0(s) = \bar{G}_n(s) \bar{G}_p(s) \bar{G}_{ts}(s), \bar{G}_2(s) = \bar{G}_{ts}(s), H_d(s) = \dfrac{f_d(s)}{d(s)}$. With the nonlinear signal in Eq. (5), the error between the outputs of the numerical and physical substructures becomes:

$$e(s) = \bar{x}_n(s) - \bar{x}_p(s) + \sigma(s) = \bar{G}_d(s) d(s) - \bar{G}_u(s) e^{-\tau s} u(s) + \sigma(s) \tag{7}$$

where $\bar{G}_d(s) = \bar{G}_1(s)$, $\bar{G}_u(s) = \bar{G}_0(s) + \bar{G}_2(s)$. Since the error signal e is comprised of three signals $\{d, u, \sigma\}$ in Eq.(7), the input signal here is assumed to be:

$$u(s) = K_d(s) d(s) + K_e(s) e(s) + K_\sigma(s) \sigma(s) \tag{8}$$

Substituting Eq. (8) into Eq. (7), the error transfer function can be expressed by:

$$e(s)=\frac{\bar{G}_d(s)-\bar{G}_u(s)e^{-\tau s}K_d(s)}{1+\bar{G}_u(s)e^{-\tau s}K_e(s)}d(s)+\frac{1-\bar{G}_u(s)e^{-\tau s}K_\sigma(s)}{1+\bar{G}_u(s)e^{-\tau s}K_e(s)}\sigma(s) \tag{9}$$

The controller transfer functions, K_d and K_σ, need to be determined so that the error becomes zero. Thus, we propose the controller transfer functions to be:

$$\begin{cases} K_d(s)=\dfrac{\bar{G}_d(s)}{\bar{G}_u(s)}F_d(s) \\ K_\sigma(s)=\dfrac{1}{\bar{G}_u(s)}F_\sigma(s) \end{cases} \tag{10}$$

where F_d and F_σ are filters to realise proper transfer functions of K_d and K_σ. When these filters can set to be 1.0 and there is no pure time delay, very accurate control with near zero-error is achievable. In this case, the controller transfer function, K_e, is not essential for the control. However, when the pure time delay is not zero, K_e becomes a key element especially for maintaining stability.

3. Dynamical substructuring system for a base-isolated structure

A base-isolated structure can be divided into two substructures, as shown in Fig. 1. The numerical substructure comprises the mass of the superstructure and the physical substructure comprises a rubber bearing. Therefore, the numerical linear model basically becomes $\bar{G}_n = G_n$, whereas the physical substructure can is $\bar{G}_p \neq G_p$.

3.1 Configuration

The equation of motion for the emulated model is expressed by:

$$m_e\ddot{x}_e(t)+f_{ec}(\dot{x}_e,t)+f_{ek}(x_e,t)=-m_e\ddot{d}(t) \tag{11}$$

where t is the time variable, x_e, m_e, f_{ec} and f_{ek} are the relative displacement, mass, force due to damping and restoring force of the emulated model, respectively.

The numerical and physical substructures in Fig. 1 are expressed as:

$$\begin{cases} m_n\ddot{x}_n(t)=f_n(t) \\ m_p\ddot{x}_p(t)+f_{pc}(\dot{x}_p,t)+f_{pk}(x_p,t)=f_p(t) \end{cases} \tag{12}$$

where f_n, x_n and m_n are the force, relative displacement and mass of the numerical substructure, respectively, while f_p, x_p, m_p, f_{pc} and f_{pk} are, respectively, the force, relative displacement, mass, force due to damping and restoring force of the physical substructure. Base on Fig. 2, the following equation is obtained:

$$f_n(t)=-f_p(t)-f_d(t) \tag{13}$$

where $f_d(t)=m_e\ddot{d}(t), m_e=m_n+m_p$.

Linear models of the substructures are now expressed by:

$$\begin{cases} \bar{m}_n\ddot{\bar{x}}_n(t)=\bar{f}_n(t) \\ \bar{m}_p\ddot{\bar{x}}_p(t)+\bar{c}_p\dot{\bar{x}}_p(t)+\bar{k}_p\ddot{\bar{x}}_p(t)=\bar{f}_p(t) \end{cases} \tag{14}$$

where $\bar{f}_n(t)\left(=-\bar{f}_p(t)-f_d(t)\right)$, $\bar{x}_n$ and $\bar{m}_n$ are the force, relative displacement and mass of the numerical linear model, and $\bar{f}_p$, $\bar{x}_p$, $\bar{m}_p$, $\bar{c}_p$ and $\bar{k}_p$ are the force, relative displacement, mass, damping coefficient and stiffness coefficient of the physical linear model.

Since the nonlinear signal can be obtained from the subtraction of the outputs of the numerical substructure and its linear model, the nonlinear signal is given as follows:

$$\ddot{\sigma}(t)=\ddot{x}_n(t)-\ddot{\bar{x}}_n(t)=-\frac{1}{\bar{m}_n}\left(f_p(t)-\bar{f}_p(t)\right) \tag{15}$$

where $m_n=\bar{m}_n$. With Eqs. (15) and (14), the force applied to the physical substructure can be expressed by:

$$f_p(t)\left(=\bar{f}_p(t)-\bar{m}_n\ddot{\sigma}(t)\right)=\bar{m}_p\ddot{\bar{x}}_p(t)+\bar{c}_p\dot{\bar{x}}_p(t)+\bar{k}_p\bar{x}_p(t)-\bar{m}_n\ddot{\sigma}(t) \tag{16}$$

Substituting Eqs. (12) and (13) into Eq. (16), the output of the numerical substructure is obtained as:

$$m_n\ddot{x}_n(t)=-\left(\bar{m}_p\ddot{\bar{x}}_p(t)+\bar{c}_p\dot{\bar{x}}_p(t)+\bar{k}_p\bar{x}_p(t)-\bar{m}_n\sigma(t)\right)-m_e\ddot{d}(t) \tag{17}$$

Here the dynamics of the transfer system is expressed by:

$$G_{TS}(s)=\frac{a}{s+a}e^{-\tau s} \tag{18}$$

where a is the transfer system coefficient. Based on this dynamics, the outputs of two substructures in Fig. 2 are found to be:

$$\begin{cases} x_n(s)=-\dfrac{\bar{m}_n+\bar{m}_p}{\bar{m}_n}d(s)-\left(\dfrac{\bar{m}_p s^2+\bar{c}_p s+\bar{k}_p}{\bar{m}_n s^2}\right)\left(\dfrac{a}{s+a}\right)e^{-\tau s}u(s)+\sigma(s) \\ x_p(s)=\left(\dfrac{a}{s+a}\right)e^{-\tau s}u(s) \end{cases} \tag{19}$$

Thus, error dynamics can be obtained from Eq. (19), as follows:

$$e(s)=-\frac{\bar{m}_n+\bar{m}_p}{\bar{m}_n}d(s)-\left[\frac{\left(\bar{m}_p+\bar{m}_n\right)s^2+\bar{c}_p s+\bar{k}_p}{\bar{m}_n s^2}\right]\left(\frac{a}{s+a}\right)e^{-\tau s}u(s)+\sigma(s) \tag{20}$$

Since Eq. (19) corresponds to Eq. (7), the following equation is obtained:

$$\bar{G}_u(s)=\left(\frac{\bar{m}_p s^2+\bar{c}_p s+\bar{k}_p}{\bar{m}_n s^2}\right)\left(\frac{a}{s+a}\right),\ \bar{G}_d(s)=-\frac{\bar{m}_n+\bar{m}_p}{\bar{m}_n} \tag{21}$$

The controller transfer functions, K_d and K_σ, can be obtained from Eqs. (21)and (10), as follows:

$$
\begin{aligned}
K_d(s) &= \frac{\bar{G}_d(s)}{\bar{G}_u(s)} = -\frac{(\bar{m}_p+\bar{m}_n)(s+a)/a}{(\bar{m}_p+\bar{m}_n)s^2+\bar{c}_p s+\bar{k}_p}s^2 \\
K_\sigma(s) &= \frac{1}{\bar{G}_u(s)} = \frac{\bar{m}_n(s+a)/a}{(\bar{m}_p+\bar{m}_n)s^2+\bar{c}_p s+\bar{k}_p}s^2
\end{aligned}
\tag{22}
$$

Following the transfer function for the error feedback action in LSC [5], we here design the transfer function K_e to be:

$$
K_e(s) = \frac{(s+a)(s+b)}{s^2+\left(\dfrac{\bar{c}_p}{\bar{m}_n+\bar{m}_p}\right)s+\left(\dfrac{\bar{k}_p}{\bar{m}_n+\bar{m}_p}\right)}\beta
\tag{23}
$$

where β is a simple controller gain .

3.2 Example: inaccurate modelling

Substructuring tests, in general, have to be conducted with an assumed model that, to one degree or another, has modelling error, because its accurate model is rarely obtained in advance of the experiments. Therefore, in this study, NLSC is numerically examined via an example of substructured test on the base-isolated structure with inaccurate parameters in the controller.

In this example, the physical substructure, demonstrating a rubber bearing, is assumed to have properties obtained by a study of LSC [5], as follows: m_p = 115 kg, c_p = 354.6 Ns/m, k_p = 158.4 kN/m. The properties of the transfer system is assumed to have a = 75.0 s^{-1} and τ = 6.0 ms, and the numerical substructure is set to be m_n = 20m_p in this study. Then, the natural frequency and damping ration of the emulated system result in ω_e = 1.29×2π rad/s and ζ_e = 0.0091, respectively.

With the above-mentioned parameters, the control signal u in NLSC for this example is expressed by:

$$
u(s) = K_{\ddot{d}}(s)\ddot{d}(s)+K_e(s)e(s)+K_{\ddot{\sigma}}(s)\ddot{\sigma}(s)
\tag{24}
$$

$$
\begin{cases}
K_{\ddot{d}}(s) = \dfrac{1}{s^2}K_d(s) = -\dfrac{2415(s+75)/75}{2415s^2+354.6s+\gamma_k 158400} \\
K_{\ddot{\sigma}}(s) = \dfrac{1}{s^2}K_\sigma(s) = \dfrac{2300(s+75)/75}{2415s^2+354.6s+\gamma_k 158400} \\
K_e(s) = \dfrac{2300(s+b)(s+75)/75}{2415s^2+354.6s+\gamma_k 158400}\beta
\end{cases}
\tag{25}
$$

where γ_k is the modelling error parameter for stiffness, k_p. Note that $K_{\ddot{d}}$ and $K_{\ddot{\sigma}}$ are the proper transfer functions related to the ground motion acceleration, $\ddot{d}$, and the nonlinear signal, $\ddot{\sigma}$. Based on the design of LSC [5], suitable parameters are found to be β = 75 and b =18.75. In addition, $K_{\ddot{d}}$ and K_e in Eq. (25) are taken as the LSC controller for the comparison with the NSLC controller.

A Japan Meteorological Agency Kobe (JMA Kobe) ground motion, recorded during the 1995 Hyogo-ken Nanbu Earthquake, is adopted as an input ground motion. Since this numerical simulation is to be compared with the experimental study in section 4, for the comparison, this input motion is scaled down to 10%, following the maximum stroke of an actuator used in the experiment. The response of the emulated system is shown in Fig. 3 and the maximum displacement reaches to 35.6 mm.

In the numerical simulations, the maximum errors of $\{x_n - x_p, x_e - x_p, x_e - x_n\}$ become {5.8 mm, 35.4 mm, 38.8 mm} in LSC and {0.3 mm, 3.2 mm, 3.2 mm} in NLSC. Although the largest error in LSC is 109% of the maximum emulated response (i.e., 35.6 mm), the largest error in NLSC is only 9.0% of the maximum emulated response. Now, NLSC is found to achieve good control even when its controller contains an inaccurate parameter.

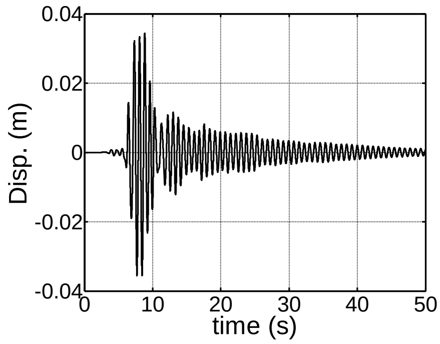

Fig. 3 – Response of the emulated system

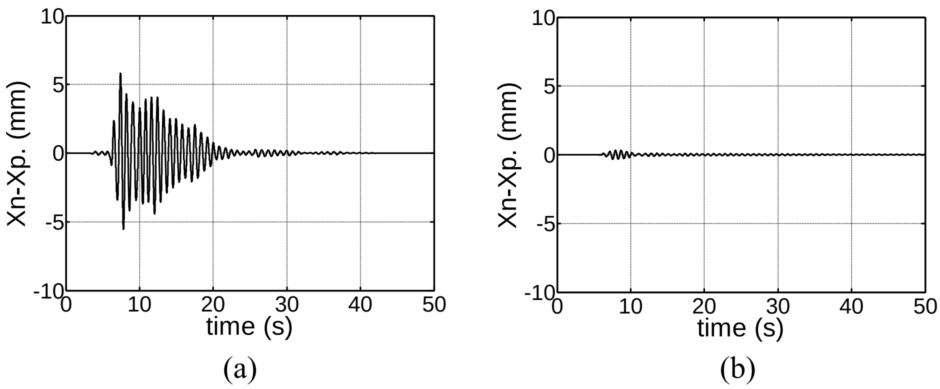

Fig. 4 – Numerical results: (a) LSC, (b) NLSC

4. Experiment

4.1 Experimental system

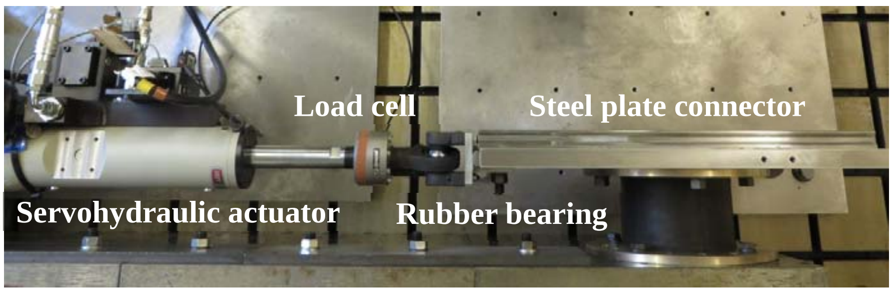

Fig. 5 – Test rig for the substructured experimet on a rubber bearing

Test rig shown in Fig. 5 was built at the University of Bristol for substructuring test on a rubber bearing. This rig comprised a ±25 kN force, ±120.0 mm stroke servohydraulic actuator and a proprietary inner-loop discrete-time controller (thus comprising the transfer system), together with a connecting steel plate and a bearing made of natural rubber (the physical substructure). In addition to the substructure control signal, the actuator was configured to additively generate earthquake ground excitations to the rubber bearing. The diameter and height of the rubber bearing were 200.0 mm and 125.0 mm, respectively, and the measured mass of the steel plate was 115 kg. Rigid connections ensured that the outputs from the LVDT displacement transducer and load cell attached to the actuator were equivalent to the displacement and force applied to the rubber bearing. DSS was implemented as an outer-loop configuration using *dSPACE* 1104 hardware, operating with a sampling interval of 1.0 ms.

Identification tests were conducted on the physical substructure and transfer system in Fig. 5 with a band-limited white noise between 0.02 × 2π and 100.0 × 2π rad/s, time duration of 120.0 s and sampling interval of 1.0 ms. The output-error method provided by the System Identification Toolbox within MATLAB was applied in this identification. Then, the properties of the physical substructure was identified to be m_p = 114.3 kg, c_p = 354.6 Ns/m and k_p = 158.4 kN/m. Similarly, the properties of the transfer system was also found to be a = 75.0 s^{-1} and τ = 6.0 ms, from the averaged best-fit first-order model of the transfer system.

4.2 Substructured test

Substructuring experiments were implemented under exactly the same conditions as the numerical example with the LSC and NLSC controllers in section 3; as inaccurate modelling, five times larger value of k_p was adopted in the controllers in the experiment. In the experimental results shown in Fig. 6, the maximum value of $x_n - x_p$ became 6.5 mm in LSC and 0.4 mm in NLSC; note that the emulated response is unknown and the errors related to x_e were not obtained here. According to the experimental results, the error obtained by NLSC is nearly 1/15 of the LSC's result. Now, the efficiency of NLSC was verified in both experimental and numerical examinations.

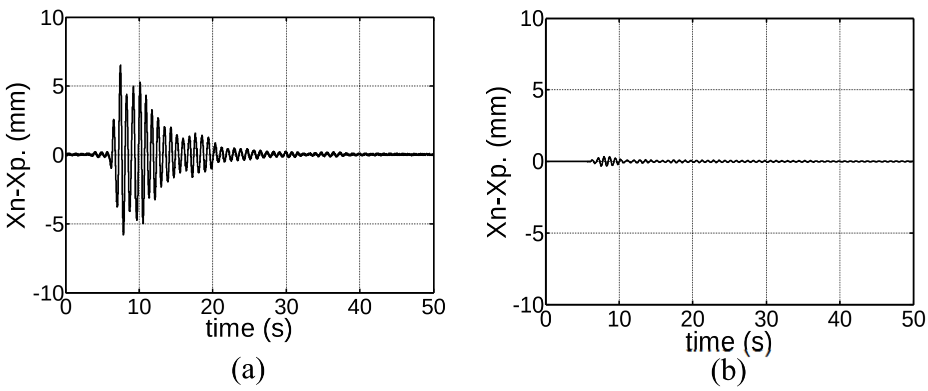

Fig. 6 – Experimental results: (a) LSC (b) NLSC

5. Conclusions

This study proposed NLSC for substructured tests based on DSS. NLSC was numerically and experimentally examined together with LSC, via a substructuring test on a rubber bearing. In the examinations, the stiffness in the rubber bearing was assumed to be five times as large as its real value in order to introduce deliberately large modelling errors in both NLSC and LSC controllers. In the numerical and exprerimental studies, NLSC succeeded in generating accurate results even with the inaccurate modelling, while LSC was unable to do so under the same condition. The efficiency and practicality of NLSC were numericallly and experimentaly verified.

6. Acknowledgements

This work has been supported by Professor David Stoten at the University of Bristol. The authors gratefully acknowledge the support of Japanese Society for the Promotion of Science (Postdoctoral Fellowships for Research Abroad, No.:20140023).

7. References

[1] Stoten DP, Hyde RA (2006): Adaptive control of dynamically substructured systems: the single-input single-output case, Proceedings of the IMechE Part I, *Journal of systems & control Engineering*, **220**(2), 63–79.
[2] Tu JY, Stoten DP, Hyde RA, Li G (2011): A state-space approach for the control of multivariable dynamically substructured systems, Proceedings of the IMechE Part I, *Journal of systems & control Engineering*, **225**(17), 935–953.
[3] Tu JY, Lin PY, Stoten DP, Li G (2010): Testing of dynamically substructured, base-isolated system using adaptive control techniques, *Earthquake Engineering and Structural Dynamics*, **39**(6), 21–42.
[4] Enokida R, Takewaki I, Stoten D (2014): A nonlinear signal-based control method and its applications to input identification for nonlinear SIMO problems, *Journal of Sound and Vibration*, **333**(24), 6607–6622.
[5] Enokida R, Stoten D, Kajiwara K (2015): Stability analysis and comparative experimentation for two substructuring schemes, with a pure time delay in the actuation system, *Journal of Sound and Vibration*, **346**, 1–16.